Supplement of Biogeosciences, 18, 135–158, 2021
https://doi.org/10.5194/bg-18-135-2021-supplement

Biogeosciences
Open Access

Supplement of

A climate-dependent global model of ammonia emissions from chicken farming

Jize Jiang et al.

Correspondence to: Jize Jiang (jize.jiang@ed.ac.uk)

1 Information of USEPA AFO's monitoring data

Table S1 Chicken housing data used for simulations. 2 houses are from each site. * data were used for deriving indoor conditions only.

Site name	Location	Production system	Monitored period
CA1B*	San Joaquin, California	Broiler (barn)	Sep 01, 2007 to Oct 31, 2009
IN2B*	Wabash, Indiana	Layer (barn)	May 15, 2008 to Mar 15, 2009
NC2B	Nash, North Carolina	Layer (barn)	Mar 15, 2008 to Mar 15, 2009

2 Parameterization of aerodynamic resistance (R_a) and boundary layer resistance (R_b)

The value of R_a, which is dependent on the stability of air, is calculated from (Seinfeld and Pandis, 2016):

$$R_a = \frac{\left[ln\left(\frac{z}{z_0}\right) - \psi_m\left(\frac{z}{L}\right)\right]^2}{k^2 u} \quad \text{(SM1)}$$

where u (m s^{-1}) is the wind speed measured at z (m) height above ground, z_0 (m) is the roughness length, L (m) is the Monin-Obukhov length, ψ_m is a stability correction function, and k is the von Karman constant.

The stability correction function is calculated for stable and unstable atmospheric conditions:

Stable conditions:

$$\psi_m\left(\frac{z}{L}\right) = -\frac{5z}{L} \quad \text{(SM2)}$$

Unstable conditions:

$$\psi_m\left(\frac{z}{L}\right) = ln\left(\frac{1+X}{2}\right)^2 + ln\left(\frac{1+X^2}{2}\right) - 2tan^{-1}(X) + \frac{\pi}{2} \quad \text{(SM3)}$$

where $X = \left(1 - 16\frac{z}{L}\right)^{\frac{1}{4}}$ (SM4)

The Monin-Obukhov length L are parameterized from:

$$L = \frac{T{u_*}^3 \rho c_p}{kgH} \quad \text{(SM5)}$$

where T (K) is the air temperature at 2 m above ground, u_* (m s^{-1}) is the friction velocity with z_0 roughness height, ρ (kg m^{-3}) is air density, c_p (J kg^{-1} K^{-1}) is the specific heat capacity of dry air, and g (m s^{-2}) is the acceleration of gravity, and H is the sensible heat flux (J m^{-2} s^{-1}). The friction velocity is calculated from:

$$u_* = \frac{ku}{ln\left(\frac{z}{z_0}\right) - \psi_m\left(\frac{z}{L}\right)} \quad \text{(SM6)}$$

R_b depends on diffusivity through the quasi laminar sub-layer, where the entrained transfer is described by the boundary layer Stanton number (B) and is approximately equal to 5 (Nemitz et al., 2000; Riddick et al., 2017):

$$R_b = (Bu_*)^{-1} \quad \text{(SM7)}$$

3 Parameterization of indoor temperature for chicken houses

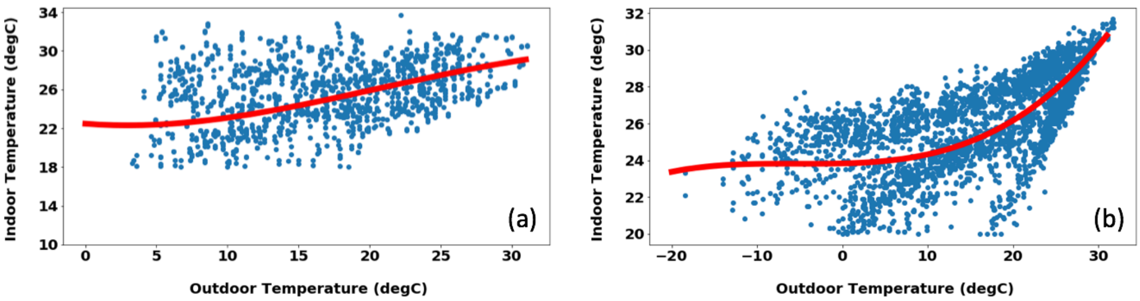

Figure S1 Modelled stable temperature in a) broiler house ($T_B = 0.00020T^3 + 0.0010T^2 + 0.024T + 22.1$), b) layer house ($T_L = 0.00014T^3 + 0.0023T^2 + 0.011T + 23.8$). The relationship for the broiler house is for data where bird bodyweight is >0.5 kg, as explained in the main text.

4 Housing resistance

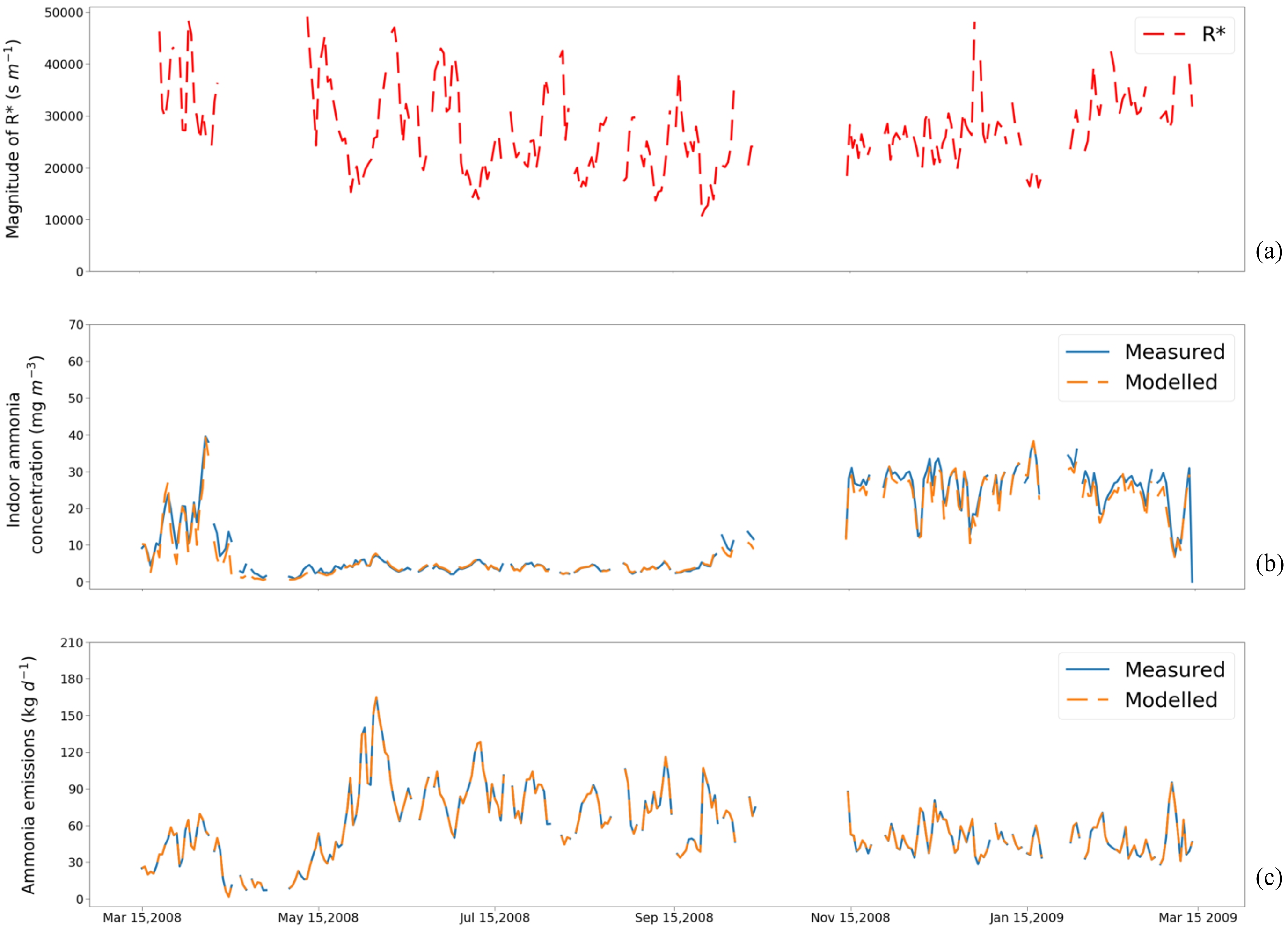

Figure S2 Site simulations using the new UA hydrolysis parameterisation for House A at site NC2B, Nash, North Carolina from March 15 to March 15, 2009. a): Inversion derived resistance values (R*). b): Comparison between measured and modelled indoor NH3 concentrations of the house. c) Comparison between modelled NH3 emissions and calculated NH3 emissions from measured indoor concentrations. The comparisons demonstrate the ability of the model to reproduce measured NH3 concentrations and emissions given the use of the fitted values of R*.

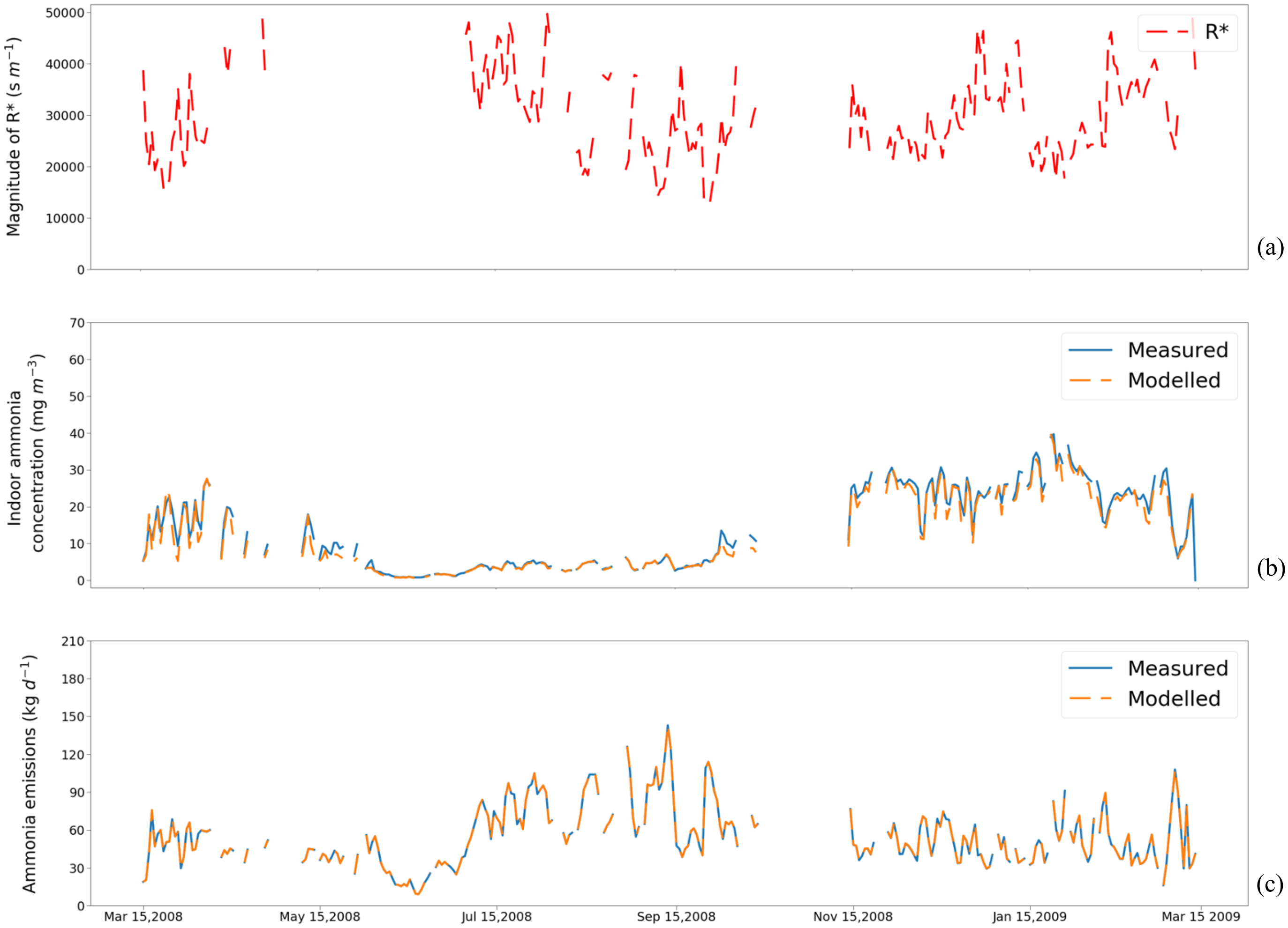

Figure S3 Site simulations using the new UA hydrolysis parameterisation for House B at site NC2B, Nash, North Carolina from March 15 to March 15, 2009. a): Inversion derived resistance values (R*). b): Comparison between measured and modelled indoor NH3 concentrations of the house. c) Comparison between modelled NH3 emissions and calculated NH3 emissions from measured indoor concentrations. The comparisons demonstrate the ability of the model to reproduce measured NH3 concentrations and emissions given the use of the fitted values of R*.

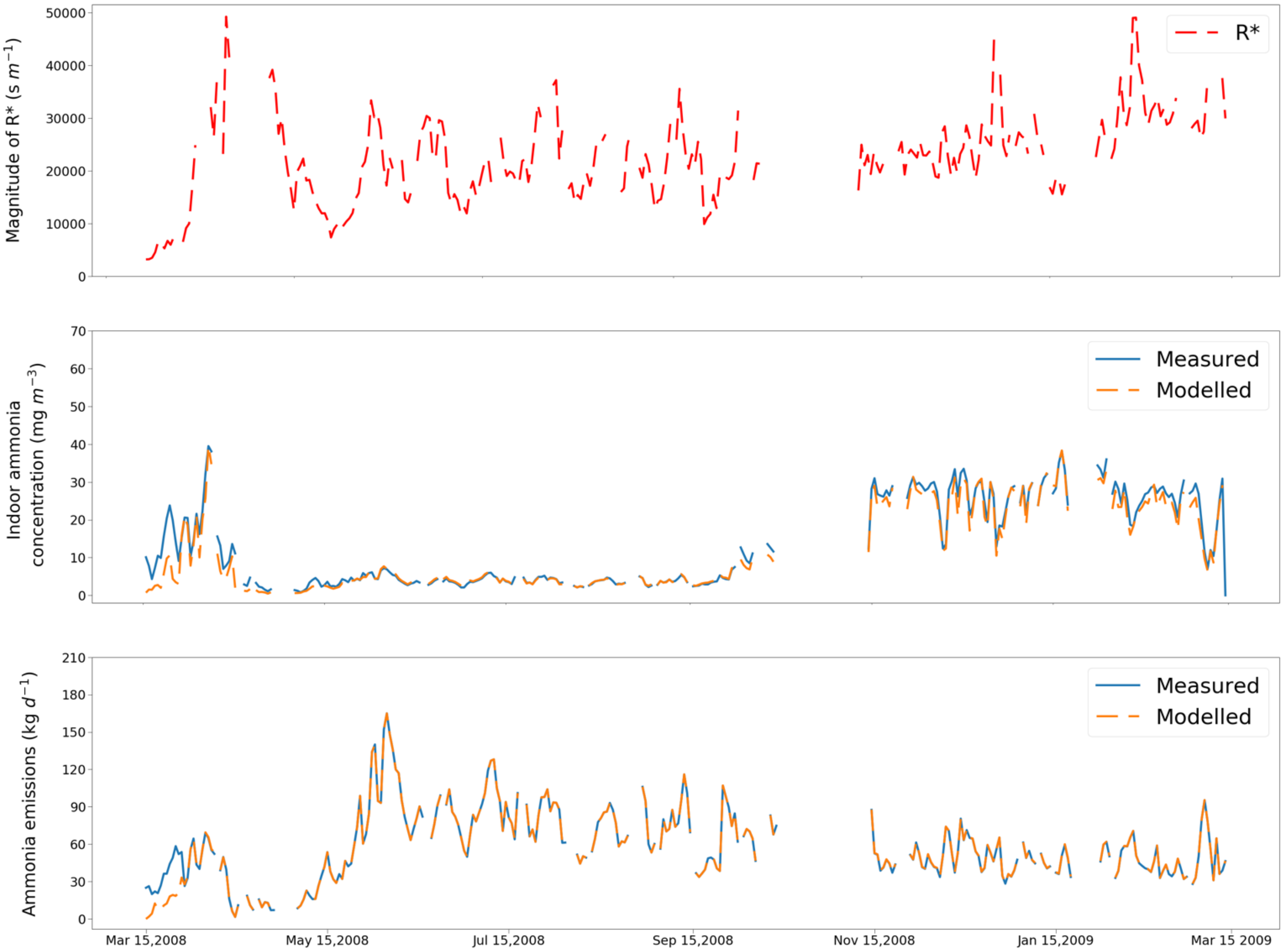

(a)

(b)

(c)

Figure S4 Site simulations using the UA hydrolysis parameterisation from the Elliot and Collins (1982) for House A at site NC2B, Nash, North Carolina from March 15 to March 15, 2009. a): Inversion derived resistance values (R*). b): Comparison between measured and modelled indoor NH3 concentrations of the house. c) Comparison between modelled NH3 emissions and calculated NH3 emissions from measured indoor concentrations. The comparisons demonstrate the ability of the model to reproduce measured NH3 concentrations and emissions given the use of the fitted values of R*.

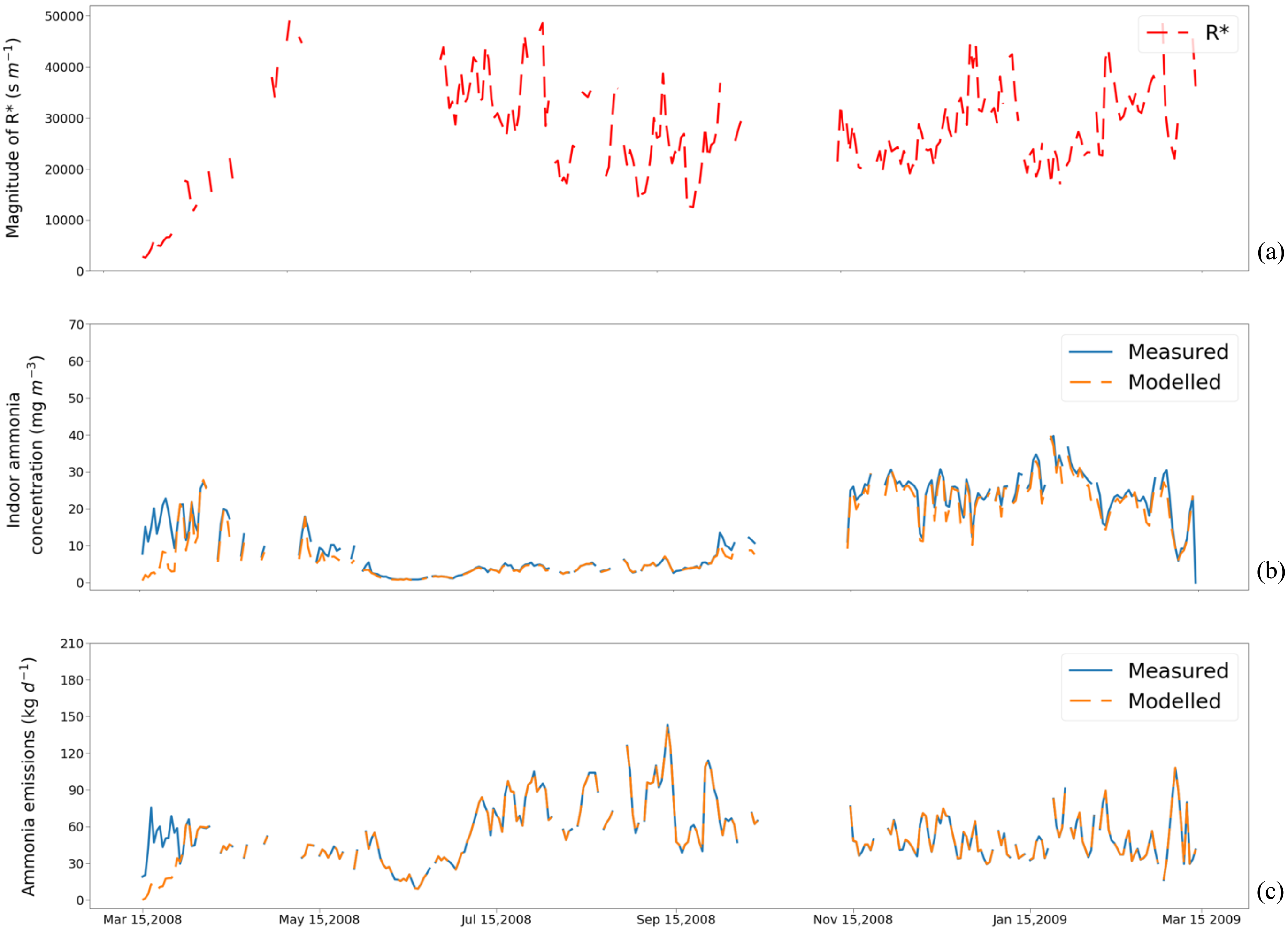

Figure S5 Site simulations using the UA hydrolysis parameterisation from the Elliot and Collins (1982) for House B at site NC2B, Nash, North Carolina from March 15 to March 15, 2009. a): Inversion derived resistance values (R*). b): Comparison between measured and modelled indoor NH3 concentrations of the house. c) Comparison between modelled NH3 emissions and calculated NH3 emissions from measured indoor concentrations. The comparisons demonstrate the ability of the model to reproduce measured NH3 concentrations and emissions given the use of the fitted values of R*.

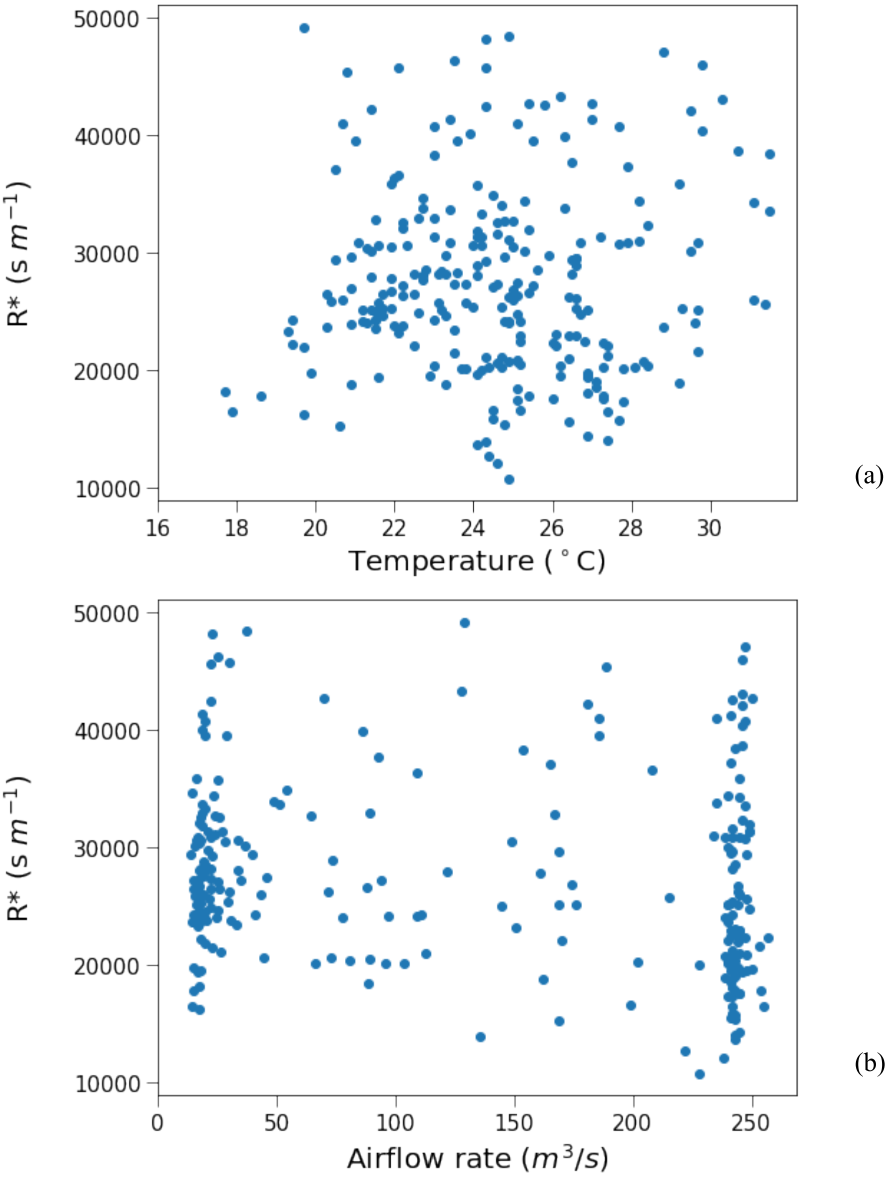

Figure S6 Consideration of possible relationships between a) temperature and b) ventilation rate with the inversion derived R* values for House A at NC2B.

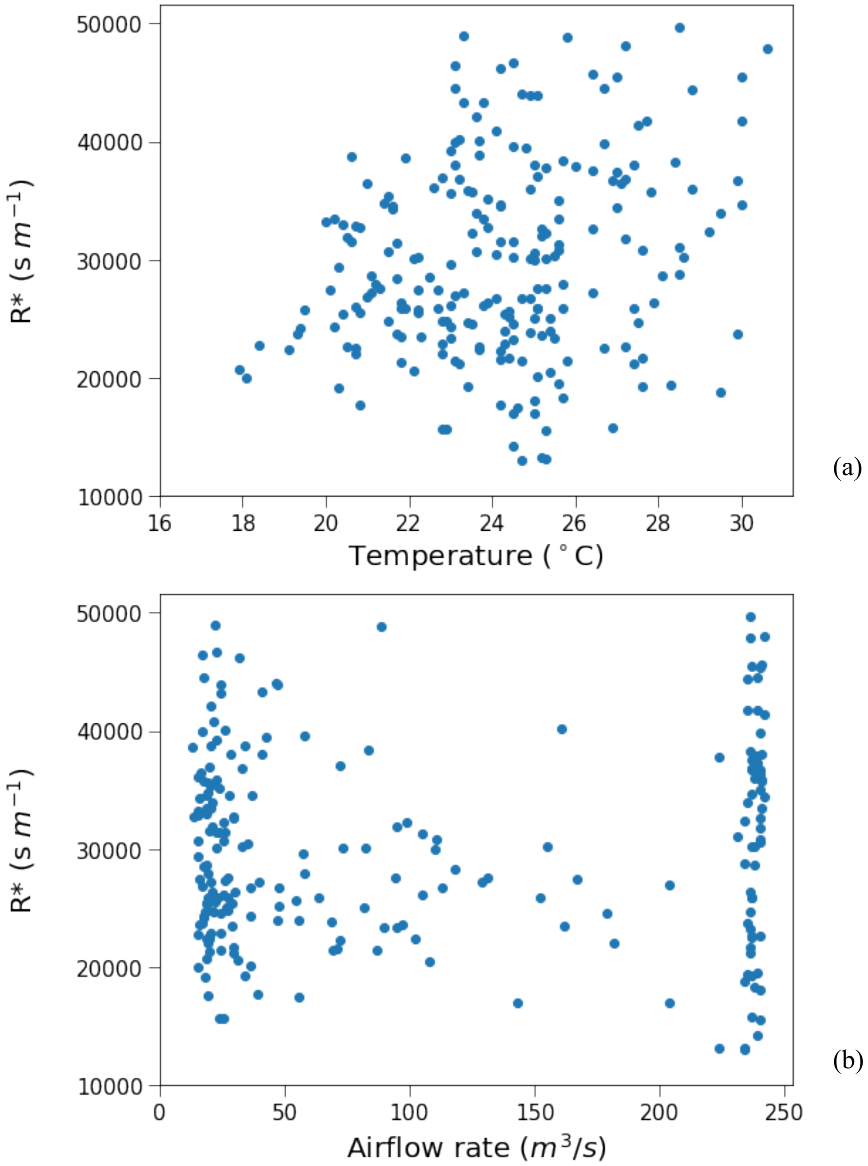

Figure S7 Consideration of possible relationships between a) temperature and b) ventilation rate compared to the inversion derived R* values for House B at NC2B.

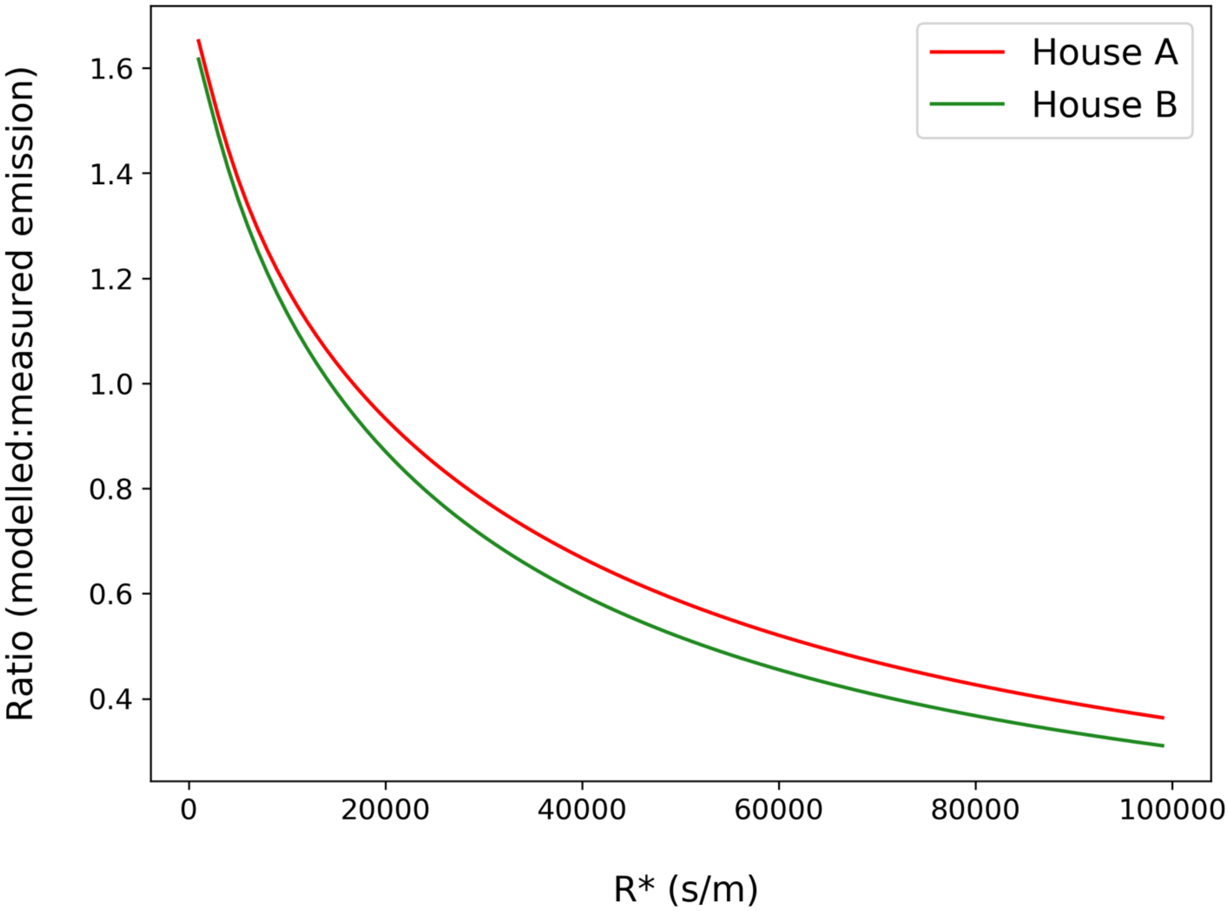

Figure S8 Ratio of total modelled and measured NH_3 emissions over the simulation period (when measurements were available) as a function of R* value for House A and House B at NC2B. The modelled values were derived by using constant R* throughout the simulation period under the same environmental conditions as chicken houses at NC2B.

5 Model configurations for site simulations of land spreading

We set the application rate to 100 kg N ha^{-1} (equivalent to 10 g N m^{-2}), which is comparable to the value used in Rodhe and Karlsson (2002) (110 kg N ha^{-1}), Sharpe et al. (2004) (109 kg N ha^{-1}, 99 kg N ha^{-1}, 133 kg N ha^{-1}) and Marshall et al. (1998) (70 kg N ha^{-1}). The model is driven by the mean daily air temperature given from the previous studies, while the diurnal variations of temperature and other meteorological factors such RH and precipitation are not available from these publications. The ground temperature is assumed to be 2 ° C higher than the air temperature, where ground temperature is not available from the published experiment. The sum of aerodynamic and boundary layer resistances is assumed to be 100 s m^{-1} as it cannot be calculated due to the lack of environmental inputs provided by the authors. The wash-off pathways of the model were shut down due to the unknown rainfall information, so the simulations are representative of rain free experimental conditions. We initialized the model simulation using a 7-day period prior to application of chicken litter, to allow initialisation for each nitrogen pools. The model was then run for 21 days to determine the NH_3 volatilization. We compared to experimental results for chicken that are broilers or layers (rather than other poultry, e.g. turkey) and data for relatively fresh litter which was stored for a short period before application, normally less than a week or 10 days.

6 Ammonia emissions from global chicken housing using new parameterization for UA hydrolysis

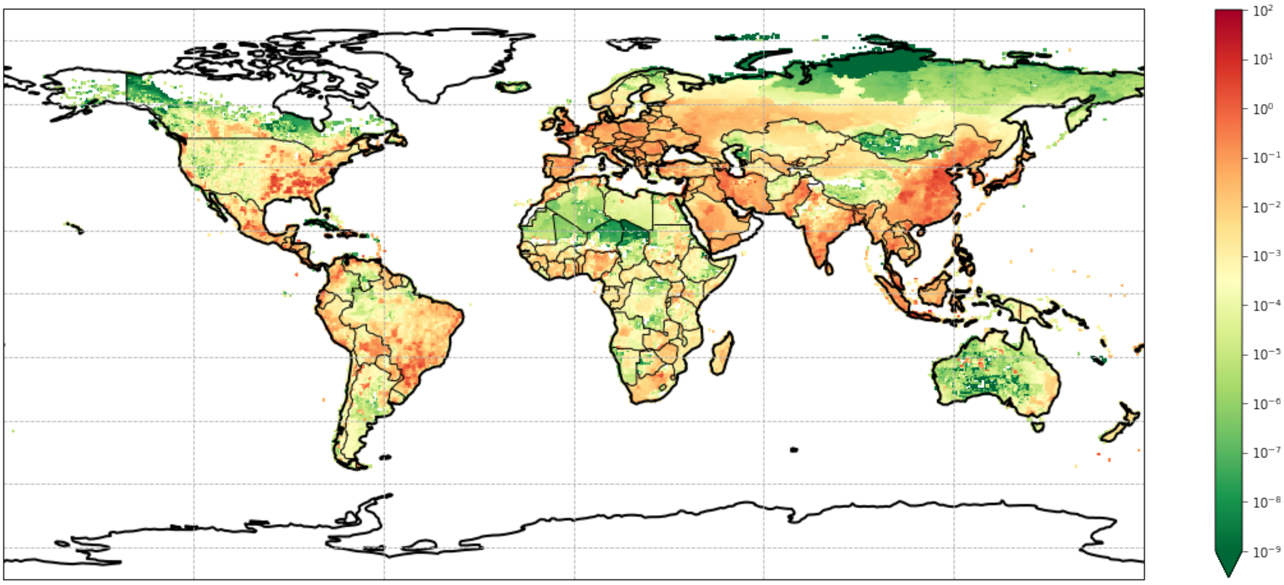

(a)

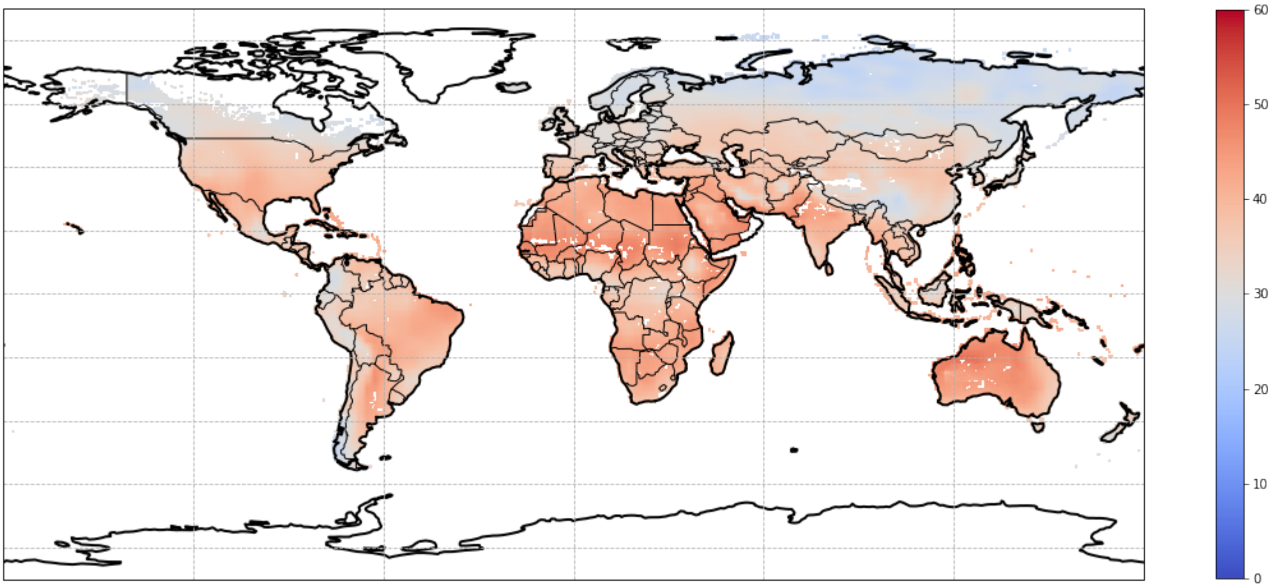

(b)

Figure S9 Simulated a) annual global NH3 emissions (Gg yr-1) from chicken housing in 2010. b) Percentage of excreted N that volatilizes (Pv, %) as NH3 from chicken housing in 2010. In both cases, these estimates show the effect of using the new parameterisations derived from the AFO's data for UA hydrolysis (Figure 3). The resolution is 0.5°×0.5°.

7 Ammonia emissions from chicken manure application for crops

Table S2 Total N application, NH_3 emission from chicken manure applications and percentage of volatilization (P_V, %) for six major crops and other crops.

Crop	N application (Gg)	NH_3 emission (Gg)	P_V (%)
Barley	273.9	97.2	35.5
Maize	1647.2	676.3	41.1
Potato	244.4	98.9	40.4
Rice	1470.7	641.2	43.6
Sugar beet	63.8	22.7	35.6
Wheat	1385.9	542.7	39.2
Other	1890.5	648.5 *	34.3 **
Total	6976.2	2727.6	39.1

NH_3 emission from other crops (*) was obtained from an average P_V (**) of the six major crops' at local area.

8 Chicken density distribution

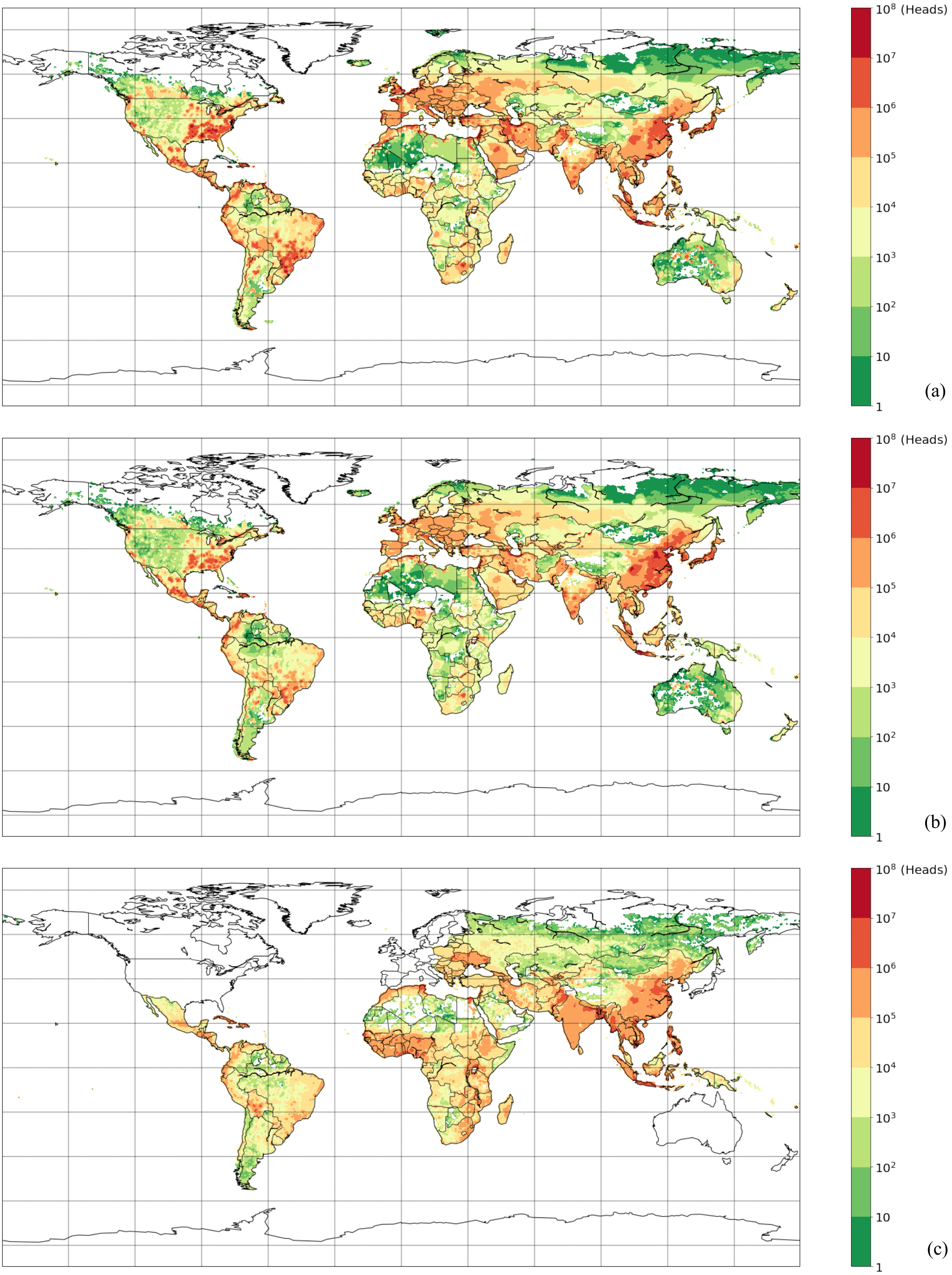

Figure S10 Global density distribution of a) broilers, b) layers, c) backyard chicken in 2010, based on FAO (2018) in a resolution of 0.083° × 0.083°.The total head is approximately 9.63×10^9 for broilers, 6.83×10^9 for layers and 3.73×10^9 for backyard chicken.

9 Estimates of uncertainty

The overall uncertainty is estimated as the square root of the sum of the squares of the individual uncertainties, expressed as mean values of magnitudes of positive and negative changes from the sensitivity tests. For housing emissions, the estimated uncertainty is 33 %, which combines uncertainty from indoor resistance on housing emissions (29 %, mean of +27.1 % and -30.6 %), manure pH (11 %, mean of -15.9 % and +5.8 %) and excreted nitrogen (12 %, mean of -12.3 % and +12.6 %). The uncertainty of emissions from chicken manure land spreading is 18 %, resulting from uncertainty in manure pH (11 %) and runoff coefficient (14 %, mean of -11.8 % and +16.5 %). The uncertainty of emissions from backyard chicken is 21 %, which combines uncertainty from excreted nitrogen (12 %), manure pH (11 %) and runoff coefficient (14 %). The total expected uncertainty in annual global emissions of NH_3 is estimated to be 22 % of the total global emissions, corresponding to 1.2 Tg N per year. This value is determined by combining all component uncertainties, i.e. indoor resistance for emissions from both housing and land spreading (together 7 %, mean of -6.4 % and +8.5 %), manure pH (11 %), runoff coefficient (14 %) and excreted nitrogen (12 %), assuming that they are independent. We estimated individual uncertainties using simple methods and combined them assuming they are independent (using the square root of the sum of the squares) to give a rough idea of the overall uncertainties on emissions. Given the relatively large inherent uncertainties and numerous assumptions in our model, we feel more detailed methods for estimating uncertainties are probably not justified.

References

Marshall, S. B., Wood, C. W., Braun, L. C., Cabrera, M. L., Mullen, M. D. and Guertal, E. A.: Ammonia Volatilization from Tall Fescue Pastures Fertilized with Broiler Litter, J. Environ. Qual., 27(5), 1125–1129, doi:10.2134/jeq1998.00472425002700050018x, 1998.

Nemitz, E., Sutton, M. A., Schjoerring, J. K., Husted, S. and Paul Wyers, G.: Resistance modelling of ammonia exchange over oilseed rape, Agric. For. Meteorol., 105(4), 405–425, doi:10.1016/S0168-1923(00)00206-9, 2000.

Riddick, S. N., Blackall, T. D., Dragosits, U., Tang, Y. S., Moring, A., Daunt, F., Wanless, S., Hamer, K. C. and Sutton, M. A.: High temporal resolution modelling of environmentally-dependent seabird ammonia emissions: Description and testing of the GUANO model, Atmos. Environ., 161, 48–60, doi:10.1016/j.atmosenv.2017.04.020, 2017.

Rodhe, L. and Karlsson, S.: Ammonia Emissions from Broiler Manure Influence of Storage and Spreading Method Lena, Biosyst. Eng., 82(4), 455–462, doi:10.1006/bioe.2002.0081, 2002.

Seinfeld, J. H. and Pandis, S. N.: Atmospheric Chemistry and Physics: From Air Pollution to Climate Change, 3rd ed., Wiley. [online], 2016.

Sharpe, R. R., Schomberg, H. H., Harper, L. A., Endale, D. M., Jenkins, M. B. and Franzluebbers, A. J.: Ammonia Volatilization from Surface-Applied Poultry Litter under Conservation Tillage Management Practices, J. Environ. Qual., 33(4), 1183, doi:10.2134/jeq2004.1183, 2004.